

SIMULATION AND ANALYSIS OF GAUSSIAN APODIZED FIBER BRAGG GRATING STRAIN SENSOR

МАТЕМАТИЧЕСКАЯ МОДЕЛЬ ДАТЧИКА НАПРЯЖЕНИЙ НА ОСНОВЕ ВОЛОКОННО-ОПТИЧЕСКОЙ БРЭГГОВСКОЙ РЕШЕТКИ С ГАУССОВЫМ ПРОФИЛЕМ

© 2012 г. К. S. Khalid, MSc; M. Zafrullah, PhD; S. M. Bilal, PhD Scholar; M. A. Mirza, PhD

E-mail: enggr_khurrain@yahoo.com, dr.zafrullah@uettaxila.edu.pk, syed.bilal@uettaxila.edu.pk, aleem.mirza@gmail.com

University of Engineering & Technology, Taxila – 47050, Pakistan

In this paper, the performance of various apodization profiles (uniform, hyperbolic tangent and gaussian) for un-chirped Fiber Bragg Grating is investigated. Apodization techniques are used to get optimized reflection spectra with high side lobe suppression. The simulations are done by solving coupled mode equations in MATLAB using transfer matrix method which explains the relationship between the guided modes. The result shows that Gaussian profile suppresses side lobe level much more efficiently than uniform and hyperbolic tangent profiles. Gaussian apodized Fiber Bragg Grating is used to indicate strain by producing wavelength shift. MATLAB and Opti-grating result gives an idea about the efficiency of the suggested scheme to analyze strain measurements by giving a linear response.

Keywords: fiber Bragg grating, coupled mode theory, coupled mode equations, transfer matrix method, apodized fiber Bragg grating, wavelength division multiplexing.

OCIS codes: 060.0060, 060.3735

Submitted 18.08.2012

Introduction

Fiber Bragg Gratings (FBGs) are those filters which works on the theory of Bragg reflection. FBGs usually reflect light in a shorter range of wavelength and transmit remaining wavelengths [1]. When light propagate through the Fiber Bragg Grating (FBG), the total reflection take place at Bragg wavelength and the remaining wavelengths are not affected by the Bragg grating except a few side lobes exist in reflection spectrum [2]. Suppression of the side lobes is important for some applications such as wavelength division multiplexing (WDM), to eliminate cross-talk between information channels. The side lobes suppression in the reflection spectrum is done by gradually changing the amplitude of the coupling coefficient along the grating length known as apodization [3]. To meet specific parameter requirements for particular FBG applications, the apodization profile can be optimized. Various apodization profiles are investigated for dispersion compensation and filter applications

[4–6]. The reflection of wavelength also depends on the strain and temperature. So FBG can be used in sensor technology. The important feature of these devices is that the sensed information i.e. the strain or temperature is translated into the wavelength, which is a key component, giving reproducible measurements in spite of optical losses and intensity fluctuations [7]. However, a problem with this type of sensors lies in the detection of the small wavelength shift in the reflected signal due to changing in strain.

The formation of FBGs is reported by Hill *et al.* [8] in 1978 at the Canadian Communications Research Centre, Canada. During an experiment which is based on the study of nonlinear effects in an optical fiber, observable light from an argon ion laser is injected into the fiber core. Spectral measurements are done indirectly by temperature & strain changing of the FBG, verified that a very narrow band FBG filter is formed through the complete 1m length of the fiber. This grating is called the Hill's grating work as a distributed reflector that coupled the counter-

propagating to the forward propagating light beams. The beam coupling provides feedback, which improves the quality of the reflected light and increases the intensity of the interference pattern, which results an increase in the refractive index at the high intensity point.

Detailed study shows that the strength of FBG is increased with the square of the light intensity. In novel experiments, laser radiation is reflected from the fiber end at 488 nm resulting in a standing wave pattern that formed a FBG. A single photon at 244 nm in the ultraviolet (UV), proved to be more effective. Meltz *et al.* [8] shows that this radiation is used to form FBG that will reflect any wavelength by illuminating the fiber through the side of the cladding with two intersecting beams of UV light. Now the period of the interference maxima and the index change is set by the angle between the beams and the UV wavelength rather than by the visible radiation which is launched into the fiber core.

Gong *et al.* [9] reported a minimum variance shift technique for wavelength detection in FBG sensors. This technique offers high detection accuracy even when the spectrum of the FBG is in partial overlap with a neighboring FBG within a WDM sensor array. Frazao *et al.* [10] came up with a new scheme for instantaneous measurement of strain and temperature using a sampled FBG based on long period structure written using the electric arc technique. Hua *et al.* [11] have successfully demonstrated the application of Fiber Bragg Grating sensors to detect the solder interconnect debonding between flip chip ball grid array and printed circuit board in four-point bend tests. Four sensors, due to their small size, were surface-mounted on the four-corners of the ball grid array substrate, about 1 mm from the solder balls that allow more sensitive strain measurement under board flexure. The measured strain data is compared with the data from strain gauge, daisy chain resistance, and dye and pry test. The preliminary results showed that the fiber sensors were capable of detecting the onset of solder joint fracture, strain relaxation, and extent of the failure.

In this paper, the performance comparison of various apodization profiles (uniform, hyperbolic tangent and gaussian) is analyzed. The parameters observed in this work are side lobe suppression and reflectivity. The apodized FBG profile with high side lobes suppression is then analyzed under strain sensor. The remainder of the paper is organized as follows. Section II presents the

fiber Bragg grating. The coupled mode theory (CMT) is introduced in this section, and transfer matrix method (TMM) is used to solve the coupled mode equations. In Section III the apodized fiber Bragg grating (AFBG) and various apodization profiles are discussed. Section IV describes AFBG under a strain sensor. Results and discussion are presented in Section V. Finally, Section VI concludes the paper.

Fiber Bragg Grating

A FBG is a periodic variation of the refractive index along a definite length of the core of an optical fiber formed by using an intense UV source through point-by-point, interferometric or phase mask technique. When light travels through the periodic regions of higher and lower refractive index inside the fiber core, it is reflected by coherent scattering from the index variations [3]. The periodic variation in the refractive index is given by the following function

$$\delta n_{\text{eff}}(z) = \bar{\delta} n_{\text{eff}}(z) \left\{ 1 + v \cos \left[\frac{2\pi}{\Lambda_0} z + \phi(z) \right] \right\}, \quad (1)$$

where z is the coordinate of light propagation along the length of FBG, $\bar{\delta} n_{\text{eff}}(z)$ is the spatially dc index change over a grating period, v is the fringe visibility of the index change, and $\phi(z)$ is the grating chirp. The CMT is used to model the FBG, which is discussed in the next section.

Coupled Mode Theory

CMT is generally used to study light propagation in a weakly coupled waveguide medium. Fiber Bragg grating is a weakly coupled waveguide structure. The basic idea behind the CMT is that the uncoupled structure modes are solved first. A linear combination of these modes is used as a testing solution to Maxwell's equations for complicated coupled structures [12]. The derived coupled mode equations can be solved analytically or numerically. The theory assumes that the field of the coupled structures may be effectively represented by a linear superposition of the modes of the unperturbed structures. In various practical cases, this assumption gives a perceptive and exact mathematical description of electromagnetic wave propagation [13–16].

In the ideal mode approximation, the transverse component of the electric field along the grating is expressed as the superposition of the

backward and forward propagation modes, as follow [17]:

$$\vec{E}_t(x, y, z, t) = \sum_j [A_j(z) \exp(i\beta_j z) + B_j(z) \exp(-i\beta_j z)] \cdot \vec{e}_{jt}(x, y) \exp(i\omega t), \quad (2)$$

Where $A_j(z)$ and $B_j(z)$ are gradually varying amplitudes of the j -th mode backward and forward respectively, whereas, $\vec{e}_{jt}(x, y)$ describes across field distribution of j -th mode, β is the propagation constant of the j -th mode and ω is angular frequency.

CMT is a special tool for obtaining quantitative information about the spectral response of FBGs. In our simulation, we consider a Bragg reflection grating in a single mode optical fiber and assume the optical fiber is weakly guiding and no energy is coupled to radiation modes. The mode evolution of $A_j(z)$ and $B_j(z)$ along the grating length L are defined in Eq. (3) and (4). R is the forward propagating wave and S is the backward propagating wave. These two waves are mutually related by the CMEs as [17]

$$\frac{dR}{dz} = i\hat{\sigma}R(z) + i\kappa S(z), \quad (3)$$

$$\frac{dS}{dz} = -i\hat{\sigma}S(z) - i\kappa R(z), \quad (4)$$

where $R(z)$ is the amplitudes of forward propagating mode and $S(z)$ is the amplitudes of backward propagating mode defined by [16]

$$R(z) = A(z) \exp(i\delta z - \phi/2), \quad (5)$$

$$S(z) = B(z) \exp(i\delta z + \phi/2). \quad (6)$$

A single mode FBG has the following relations [17]:

$$\hat{\sigma} = \delta + \sigma - \frac{1}{2} \frac{d\phi}{dz}, \quad (7)$$

$$\kappa = \frac{\pi}{\lambda} v \bar{\delta} n_{\text{eff}}(z), \quad (8)$$

$$\sigma = \frac{2\pi}{\lambda} \bar{\delta} n_{\text{eff}}(z), \quad (9)$$

$$\delta = 2\pi n_{\text{eff}} \left(\frac{1}{\lambda} - \frac{1}{\lambda_B} \right). \quad (10)$$

The parameter $\hat{\sigma}$ is a “dc” self coupling coefficient, κ is an “AC” coupling coefficient, σ is a “DC” coupling coefficient and δ is a detuning, respectively. For unchirped FBG the parameter

$\frac{1}{2} \frac{d\phi}{dz} = 0$. In this work the illustrious transfer matrix method (TMM) is used to solve the CMEs and to get the spectral response of the FBG, explained in the next section.

Transfer Matrix Method

TMM is a flexible technique for determining the input and output fields of the FBG. In TMM, the grating of length L is divided into N short uniform sections, each section is characterized by a 2×2 matrix. By multiplying all the matrices, a global matrix representing the entire grating is obtained. The greatest advantage of this technique lies in its flexibility to be used for both uniform and non-uniform gratings. The accuracy of TMM depends on the number of sections N used the analysis. A large value of M implies a higher accuracy [18–19].

Fig. 1 demonstrates how the TMM is applied to uniform and non-uniform gratings. As stated earlier that in the implementation of TMM, each section is characterized by a unique matrix containing information specific to the section. This makes it possible to apply the technique to non-uniform grating such as apodized gratings discussed in the next section.

The transfer matrix of the individual i -th section is assumed to be given by T_i , which satisfies the following relation:

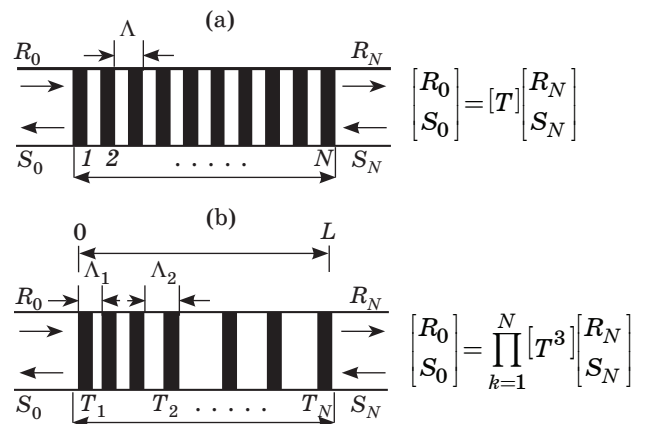


Fig. 1. Illustration of the grating using transfer matrix method. a – uniform grating, b – non-uniform grating.

$$\begin{bmatrix} R_i \\ S_i \end{bmatrix} = T_i \begin{bmatrix} R_{i+1} \\ S_{i+1} \end{bmatrix} = \begin{bmatrix} T_{11}^i & T_{12}^i \\ T_{21}^i & T_{22}^i \end{bmatrix} \begin{bmatrix} R_{i+1} \\ S_{i+1} \end{bmatrix}, \quad (11)$$

where

$$T_{11}^i = T_{22}^{i*} = \cosh(\gamma_B \Delta z_i) - i \frac{\hat{\sigma}}{\gamma_B} \sinh(\gamma_B \Delta z_i), \quad (12)$$

$$T_{12}^i = T_{21}^{i*} = -i \frac{\kappa}{\gamma_B} \sinh(\gamma_B \Delta z_i) \quad (13)$$

are the solutions to the coupled mode equation for the i -th section. The coupling coefficient $\hat{\sigma}$ and κ are the local values of the segment i -th, Δz is the section length, and γ_B is defined by

$$\gamma_B = \sqrt{\kappa^2 + \hat{\sigma}^2}. \quad (14)$$

The entire transfer relation through the sections can then be described by

$$\begin{bmatrix} R_0 \\ S_0 \end{bmatrix} = \prod_{i=1}^N [T_i] \begin{bmatrix} R_N \\ S_N \end{bmatrix} = [T] \begin{bmatrix} R_N \\ S_N \end{bmatrix}. \quad (15)$$

The transfer matrix of the whole grating T can be expressed as

$$[T] = [T_N][T_{N-1}] \dots [T_3][T_2][T_1]. \quad (16)$$

As the boundary condition, $R(0)$ is normalized to 1 and the reflected field amplitude at the output of the grating $S(N)$ is zero. The reflectivity and transmissivity of the whole grating is expressed by

$$R = \frac{T_{21}}{T_{11}}, \quad (17)$$

$$T = \frac{1}{T_{11}}. \quad (18)$$

Apodized Fiber Bragg Grating

The spectral response of a grating with a uniform index modulation along the fiber length has harmonics on the sides of the main lobe which are undesirable and may be suppressed by the procedure called apodization. Apodization is a variation of the modulation depth along the grating length. The apodized fiber Bragg grating plays an important role in order to suppress the side lobes while maintaining the reflectivity and narrow bandwidth. The side lobes are due to multiple reflections at the grating ends. From Eq. (1) $\bar{\delta}n_{\text{eff}}(z)$ can be assumed to have different apodization profiles defined by

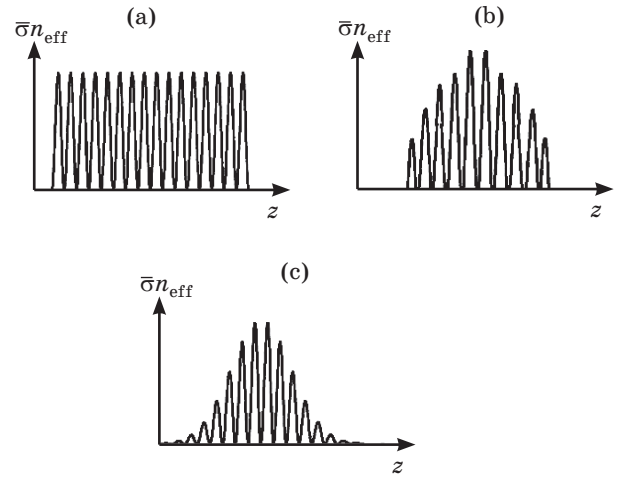


Fig. 2. Refractive Index modulation peak of different apodization profiles. a – uniform (non-apodized) index change, b – tangent hyperbolic apodized index change, c – Gaussian apodized index change.

$$\bar{\delta}n_{\text{eff}}(z) = \bar{\delta}n_{\text{eff}} f(z), \quad (19)$$

where $\bar{\delta}n_{\text{eff}}$ is the refractive index modulation peak and $f(z)$ is the apodization profile.

Apodization profiles investigated in this work are Uniform, Hyperbolic Tangent and Gaussian profile, as defined by

1. Uniform (no apodization)

$$f(z) = 1, \quad (20)$$

2. Hyperbolic Tangent

$$f(z) = \tanh(s \cdot z/L) \cdot \tanh\left[s \cdot \left(1 - \frac{z}{L}\right)\right] + 1 - \tanh^2(s/2), \quad (21)$$

3. Gaussian

$$f(z) = \exp\left\{-4 \cdot \log(2) \cdot \left[\frac{(z-L/2)^2}{s \cdot L}\right]^2\right\}, \quad (22)$$

where L is the grating length, z is the coordinate of light propagation along the length of FBG and s is taper parameter used for fine tuning of reflection spectrum.

The variation of the refractive index change along the fiber axis determines the optical properties of FBG. The refractive index modulation peak of various profile apodization profiles is shown in fig. 2.

Apodized Fiber Bragg Grating As Strain Sensor

Strain in any material is the fractional increase in its physical length when stressed.

In linear form, strain is equal to the ratio of the applied stress divided by Young's modulus of the material. The strain variation in the grating portion is determined by the wavelength shift from the sensor. According to the Bragg's law, the reflected wavelength is determined as

$$\lambda_B = 2n_{\text{eff}}\Lambda, \quad (23)$$

where n_{eff} the effective is refractive index and Λ is the grating period of the index modulation. For measuring strains it is necessary to introduce a mechanism that relates the change of strains to the change of core refractive index and the grating period.

$$n'_{\text{eff}} = n_{\text{eff}} - \frac{1}{2}n_{\text{eff}}^3\varepsilon[p_{12} - \mu(p_{11} + p_{12})], \quad (24)$$

$$\Lambda' = \Lambda[1 + (1 - P)] \cdot \varepsilon, \quad (25)$$

where n'_{eff} is the modified refractive index, Λ' is the modified grating period, ε is the axial strain along the fiber and P is an effective strain optic coefficient i.e.

$$P = \frac{n_{\text{eff}}^2}{2}[p_{12} - \mu(p_{11} + p_{12})], \quad (26)$$

p_{11} & p_{12} are strain optic tensor components, and μ is Poisson's ratio of the fiber. For a standard germane-silicate fiber $p_{11} = 0.113$, $p_{12} = 0.252$, $\mu = 0.17$, and $n_{\text{eff}} = 1.458$.

Hence the updated Bragg wavelength will become

$$\lambda_B = 2n'_{\text{eff}}\Lambda'. \quad (27)$$

The amount of the mechanical strain ($\Delta L/L$) is calculated by the variations in the Bragg wavelength shift can be expressed by the following equation [20]:

$$\lambda'_B = \lambda_B(1 - P)\varepsilon, \quad (28)$$

where λ'_B is the Bragg wavelength shift. The above equation shows that the wavelength shift is proportional to the axial strain of the fiber. A wavelength shift is calculated by putting the different values of strain varying from 100 $\mu\varepsilon$ to 800 $\mu\varepsilon$ and giving the linear response in fig. 7 and 8.

Results & Analysis

In this paper MATLAB codes are written to solve CMEs for the analysis of AFBG strain sensor. The simulations are done by assuming that the AFBG is inscribed into standard telecommunication single-mode optical fiber of $L = 20$ mm and $n_{\text{eff}} = 1.458$. Bragg wavelength is set at 1545.5 nm. MATLAB and Opti-grating (version 4.2) from Opti-wave are used for simulation purpose. The results of various apodization profiles are simulated in MATLAB and verified by the standard software of Opti-grating. The apodization profile with high side lobe suppression is then analyzed under strain sensor in order to get the better wavelength shift.

Apodized Fiber Bragg Grating Results

The plot of various apodization profiles is drawn between wavelength and reflectivity. Fig. 3 shows the graph of uniform (non-apodized) grating both in MATLAB and Opti-grating.

Simulation shows that the main lobe keeps 80% of reflected light power. Strength of side lobes in the reflectivity spectra of uniform FBG plotted in MATLAB is same as compare to that of Opti-grating plot. Fig. 4 shows the graph of

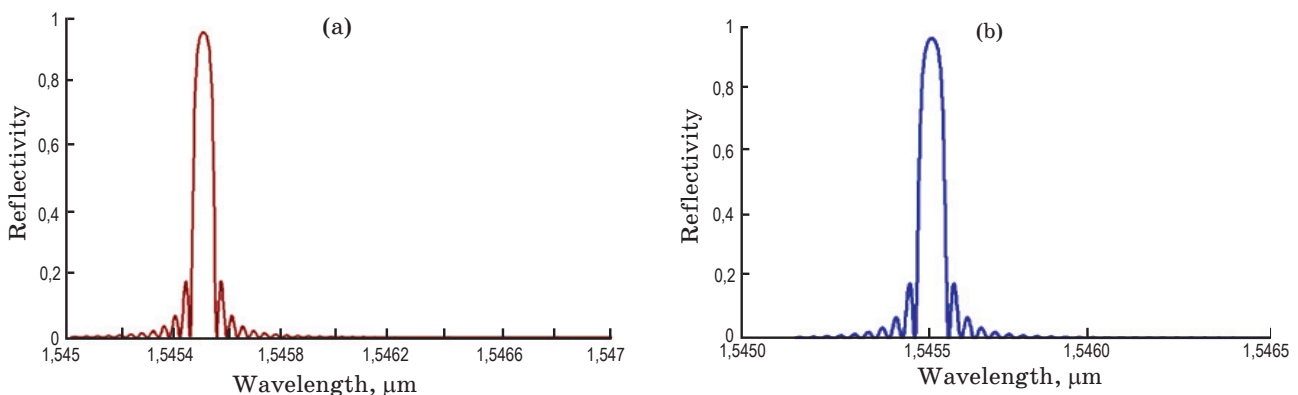


Fig. 3. Uniform gratings. a – MATLAB, b – Opti-grating.

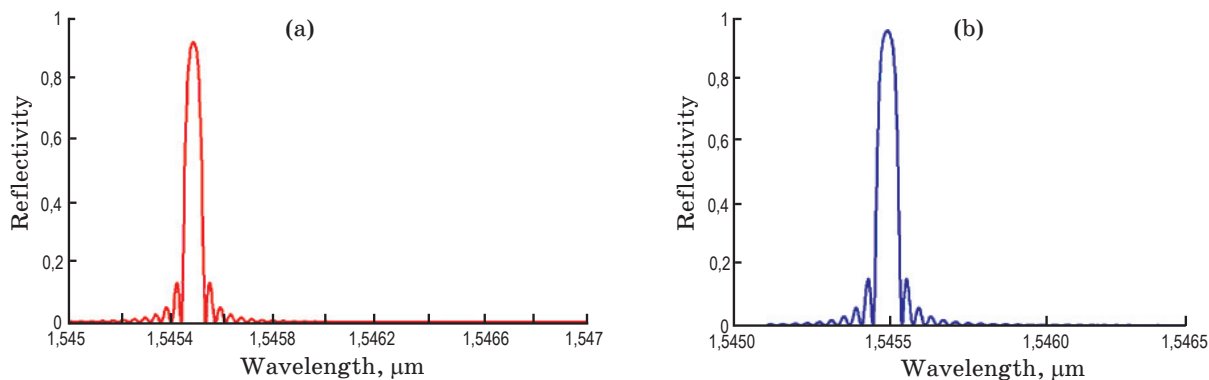


Fig. 4. Tangent hyperbolic apodized gratings. a – MATLAB, b – Opti-grating.

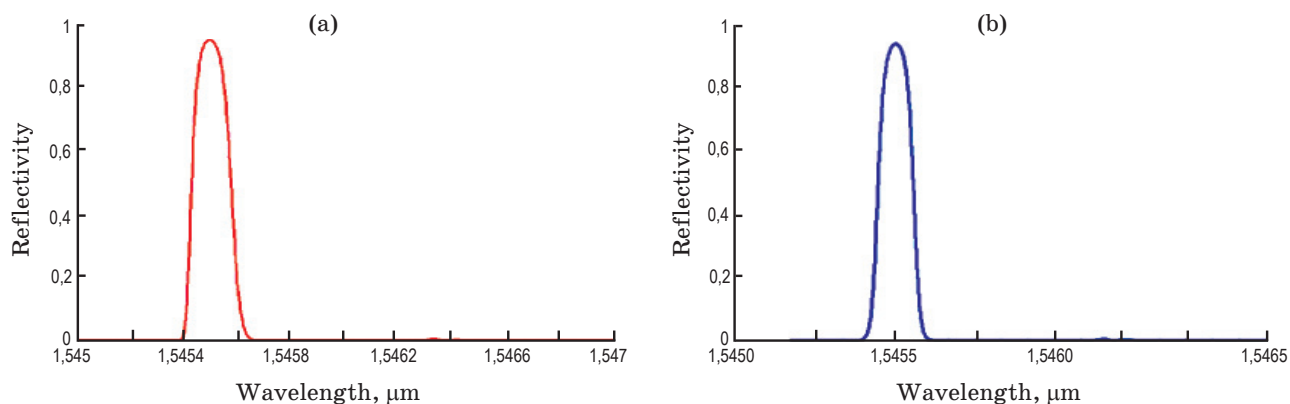


Fig. 5. Gaussian apodized gratings. a – MATLAB, b – Opti-grating.

tangent hyperbolic grating both in MATLAB and Opti-grating.

Simulation shows that the main lobe keeps 85% of reflected light power. Strength of side lobes is decreased in reflectivity spectra of tangent hyperbolic apodized FBG and an excellent agreement of MATLAB results with Opti-grating results is observed.

Fig. 5 shows the graph of Gaussian apodized grating both in MATLAB and Opti-grating.

Simulation shows that the main lobe keeps 100% of reflected light power. Strength of side lobes is completely minimized in reflectivity spectra of Gaussian apodized FBG and an excellent agreement of MATLAB results with Opti-grating results is observed.

Apodized Fiber Bragg Grating with Strain Sensor Results

MATLAB codes are written to solve CMEs for the analysis of Gaussian AFBG under strain sen-

sor. The MATLAB & Opti-grating plot of Gaussian AFBG under strain sensor is drawn between the Bragg wavelength shift and reflectivity, calculated by putting the different values of applied strain varying from 100 $\mu\epsilon$ to 800 $\mu\epsilon$ as shown in fig. 6.

The parameter observed in the graphs is the Bragg wavelength shift under various strains. The results show that an excellent match of MATLAB results with Opti-grating results is observed.

Bragg Wavelength Shift

The MATLAB and Opti-grating values of Bragg wavelength shift are obtained against applied strain by using Eq. (28) and are given in table. The graphs are plotted between the applied strain versus Bragg wavelength shift shown in fig. 7 and 8.

In MATLAB plot, a fine linear response is seen among applied strain and Bragg wavelength shift through the calculated region.

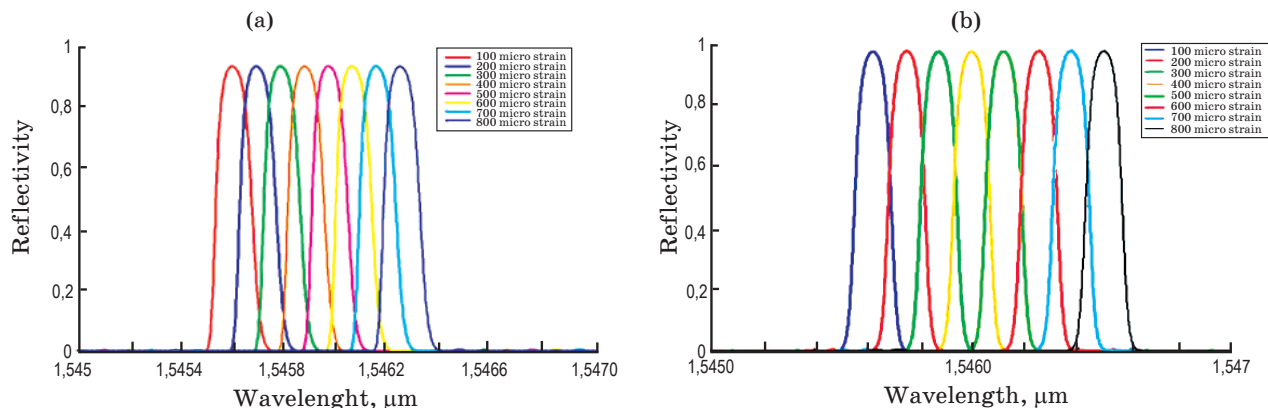


Fig. 6. Various Applied Strains. a – MATLAB, b – Opti-grating.

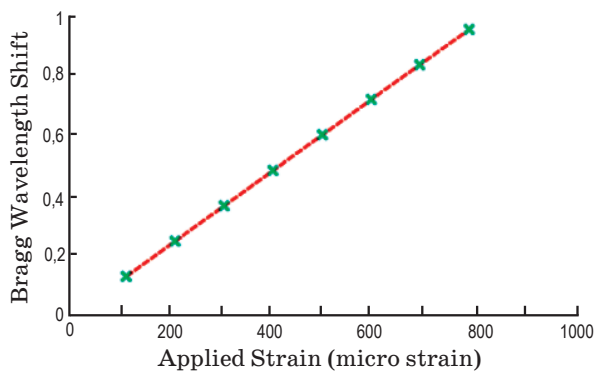


Fig. 7. Applied Strain vs Bragg wavelength shift (MATLAB).

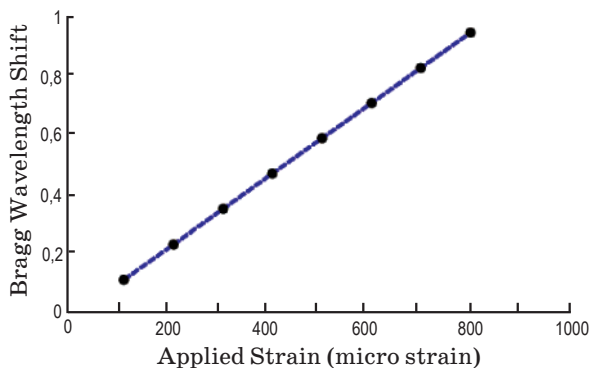


Fig. 8. Applied Strain vs Bragg wavelength shift (Opti-grating).

Applied Strain and Bragg wavelength Shift

Strain, $\mu\epsilon$	100	200	300	400	500	600	700	800
Wavelength Shift, nm (MATLAB)	0.12335	0.24672	0.37010	0.49351	0.61693	0.74034	0.86378	0.98724
Wavelength Shift, nm (Opti-grating)	0.12336	0.24673	0.37012	0.49354	0.61697	0.74041	0.86387	0.98734

In Opti-grating plot, a fine linear response is seen among applied strain and Bragg wavelength shift through the calculated region.

Comparison of MATLAB and Opti-grating Results

Single mode FBG sensors are used in the present study. Strain measurements in AFBG sensor are conducted through MATLAB coding. A comparison plot of the MATLAB and Opti-grating values of applied strain versus Bragg wavelength shift are shown in fig. 9. The typical difference of wavelength shift between MATLAB and Opti-grating value is 0.001 nm and a superb match

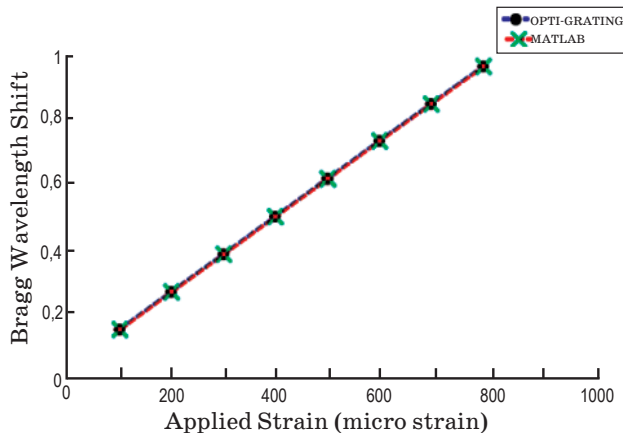


Fig. 9. Applied Strain vs Bragg wavelength shift (MATLAB & Opti-grating).

of MATLAB results with Opti-grating results is observed.

Conclusion

In this research work, the performances of FBG of several apodization profiles have been compared in terms of side lobe suppression in reflected wavelength spectra. Suppression of the side lobes is important in order to eliminate crosstalk between information channels. Power is also wasted because of these side lobes. Simula-

tion results shows that the strength of side lobes is completely minimized in reflectivity spectra of Gaussian AFBG and an excellent agreement of MATLAB results with Opti-grating results is observed. The Gaussian profile with high side lobe suppression is then used for strain sensing applications. In conclusion, the Gaussian AFBG sensor provide superior solution in detection of the small wavelength shift in the reflected signal due to strain changes, providing reproducible measurements despite optical losses and intensity fluctuations.

* * * * *

REFERENCES

1. Singh J., Khare A., Kumar S. Fiber Bragg grating modeling, characterization and optimization with different index profiles // International Journal of Engineering Science and Technology. 2010. V. 2. № 9. P. 4463–4468.
2. Singh J., Khare A., Kumar S. Design of Gaussian apodized fiber Bragg grating and its applications // International Journal of Engineering Science and Technology. 2010. V. 2. № 5. P. 1419–1424.
3. Ugale S.P., Mishra V. Optimization of fiber Bragg grating length for maximum reflectivity // IEEE Intern. Conf. on Communications and Signal Processing (ICCSP). 2011. P. 28–32.
4. Rebola J.L., Cartazo A.V.T. Performance optimization of Gaussian apodized fiber Bragg grating filters in WDM systems // Journal of Lightwave Technology. 2002. V. 20. № 8. P. 1537–1544.
5. Sahu P.K., Kumar S., Gowre C., Mahapatra S., Biswas J.C. Numerical modeling and simulation of fiber Bragg grating based devices for all-optical communication network // IFIP Intern. Conf. on Wireless and Optical Communications Networks. 2006.
6. Sun N.H., Liao J.J., Kiang Y.W., Lin S.C., Ro R.Y., Chiang J.S., Chang H.W. Numerical analysis of apodized fiber Bragg gratings using coupled mode theory // Progress in Electromagnetics Research. 2009. V. 99. P. 289–306.
7. Tahir B.A., Ali J., Rahman R.A. Strain measurements using fibre Bragg grating sensor // Am. J. Appl. Sci. (Special Issue). 2005. P. 40–48. ISSN. 1546-9239.
8. Hill K.O., Meltz G. Fiber Bragg grating technology fundamentals and overview // Journal of Lightwave Technology. 1997. V. 15. № 8. P. 1263–1274.
9. Gong J.M., MacAlpine J.M.K., Chan C.C., Jin W., Zhang M., Liao Y.B. A novel wavelength detection technique for fiber Bragg grating sensors // IEEE Photonics Technology Letters. 2002. V. 14. № 5. P. 678–680.
10. Frazao O., Romero R., Rego G., Marques P.V.S., Salgado H.M., Santos J.L. Sampled fiber Bragg grating sensors for simultaneous strain and temperature measurement // Electronics Letters. 2002. V. 38. № 14. P. 693–695.
11. Lu H., Hussain R., Zhou M., Gu X. Fiber Bragg grating sensors for failure detection of flip chip ball grid array in four-point bend tests // IEEE Sensors Journal. 2009. V. 9. № 4. P. 457–463.
12. Carvalho J.C.C., Sousa M.J., Sales C.S., Junior, Costa J.C.W.A., Frances C.R.L., Segatto M.E.V. A new acceleration technique for the design of fibre gratings // Opt. Exp. 2006. V. 14. № 2. P. 10715–10725.
13. Phing H S., Ali J., Rahman R.A., Tahir B.A. Fiber Bragg grating modeling, simulation and characteristics with different grating lengths // Journal of Fundamental Sciences. 2007. V. 3. № 2. P. 167–175.
14. Othonosa A. Fiber Bragg gratings // Review of Scientific Instruments. 1997. V. 68. № 12. P. 4309–4341.
15. Kang L.H., Kim D.K., Han J.H. Estimation of dynamic structural displacements using fiber Bragg grating strain sensors // Journal of Sound and Vibration. 2007. V. № 3. P. 534–542.

16. *Kanga D.H., Park S.O., Hong C.S., Kim C.G.* The signal characteristics of reflected spectra of fiber Bragg grating sensors with strain gradients and grating lengths // *NDT&E International*. 2005. V. 38. № 8. P. 712–718.
 17. *Yulianti I., Supa'at A.S.M., Idrus S.M., Al-hetar A.M.* Simulation of apodization profiles performances for unchirped fiber Bragg gratings // *IEEE Intern. Conf. on Photonics (ICP)*. 2010. P. 1–5.
 18. *Erdogan T.* Fiber grating spectra // *Journal of Lightwave Technology*. 1997. V. 15. № 8. P. 1277–1294.
 19. *Prabhugoud M., Peters K.* Modified transfer matrix formulation for Bragg grating strain sensors // *Journal of Lightwave Technology*. 2004. V. 22. № 10. P. 2302–2309.
 20. *Meltz G., Morey W.W.* Bragg grating formation and germanosilicate fiber photosensitivity // *Intern. Workshop on Photo induced Self-Organization Effects in Optical Fiber*. Quebec City, Quebec, 1991. *Proc. SPIE*. V. 1516. P. 185–199.
-